Organic Chemistry on Cold Molecular Films: Kinetic Stabilization of S_N1 and S_N2 Intermediates in the Reactions of Ethanol and 2-Methylpropan-2-ol with Hydrogen Bromide

Seong-Chan Park,[b] Kye-Won Maeng,[b] and Heon Kang*[a]

Abstract: We prepared thin molecular films of ethanol and 2-methylpropan-2-ol on Ru(001) substrates at temperature of 100–150 K and examined their reactivity toward HBr. The reaction intermediates and products formed at the surfaces were unambiguously identified by the techniques of Cs^+ reactive ion scattering (RIS) and low-energy sputtering. The reaction on the ethanol surface produced protonated ethanol, which is stabilized on the surface and does not proceed to further reactions. On the 2-methylpropan-2-ol surface, protonated alcohol [$(CH_3)_3COH_2^+$] and carbocation [$(CH_3)_3C^+$] were formed with the respective yield of 20 and 78%. Alkyl bromides, which are the final products of the corresponding reactions in liquid solvents, have extremely small yields on these surfaces (< 0.3% for ethyl bromide and 2% for *tert*-butyl bromide). The results indicate that the reactions on frozen films are characterized by kinetic control, stabilization of ionic intermediates (protonated alcohols and *tert*-butyl cation), and effective blocking of the charge recombination steps in S_N1 and S_N2 paths. The implication of these findings for the molecular evolution process in interstellar medium is also discussed.

Keywords: alcohols · ice · mass spectrometry · surface analysis · reaction intermediates

Introduction

Reactions on frozen molecular solids have received increasing attention in recent years partly owing to discovery that they play an important role in atmospheric and interstellar chemical processes. On ice particles in the polar stratospheric clouds, heterogeneous catalytic reactions take place which cause the seasonal recurrence of ozone depletion over the Antarctic.[1–3] Interstellar icy grains are thought to be a catalyst in extraterrestrial organics formation. The increasing evidence[4, 5] from both infrared astronomic observations[6, 7] and laboratory experiments,[8–10] support the possibility that simple chemicals are transformed to more complex molecules in the cold icy mantle of interstellar grains. The keen interest on such environmental issues has stimulated a large number of projects on the chemistry on water-ice surfaces, which include spectroscopic investigations of molecular states on ice,[11–17] laboratory model studies of the stratospheric reactions of halogen reservoir molecules ($ClONO_2$, HCl, and HBr),[18–21] reactions induced by photons[8–10] and high-energy particles,[22–24] and the measurements of fundamental chemical properties on well-defined ice films such as the mobility of water[25, 26] and proton,[27] and the proton transfer efficiency in the H_3O^+/NH_3 system.[28] The next interesting system in this line of investigation is a solid alcohol surface. Methanol is the most abundant organic molecule observed in the interstellar medium and in cometary volatiles,[5] not to mention the wide usage of alcohols as reagents and reaction media in organic chemistry laboratory. The study of solid-phase alcohols, however, has been very limited so far. The structure and phase-transition behaviors of simple alcohols such as ethanol have been examined in a frozen bulk state,[29, 30] although the surface structure and reactivity are almost completely unknown at present. Roberts et al.[31] recently examined the chlorine substitution reaction of 2-methylpropan-2-ol on a water-ice surface using temperature-programmed desorption mass spectrometry (TPDMS).

Apart from the importance to interstellar chemistry, the frozen alcohol surface is an interesting research subject from a standpoint of fundamental chemistry as well. Consider, for example, Scheme 1 which depicts reactions of hydrogen halide with ethanol and 2-methylpropan-2-ol in a liquid phase, textbook examples of the S_N1 and S_N2 reaction pathways. The reactions readily occur in ordinary solvents at room temperature and their behavior is governed by thermo-

[a] Prof. Dr. H. Kang
School of Chemistry, Seoul National University
Seoul, Kwanak-gu 151-742 (Republic of Korea)
Fax: (+82)-2-889-8156
E-mail: surfion@snu.ac.kr

[b] S.-C. Park, K.-W. Maeng
Department of Chemistry
Pohang University of Science and Technology
Pohang, Geongbuk 790-784 (Republic of Korea)

  0947-6539/03/0908-1706 $ 20.00+.50/0

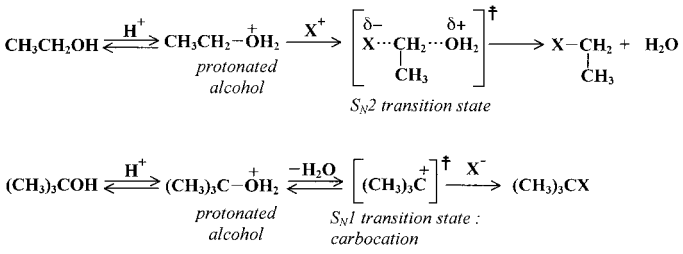

Scheme 1. Reactions of hydrogen halide with ethanol and 2-methylpropan-2-ol in a liquid phase.

dynamics. Intermediate species of the reactions such as protonated alcohol and carbocation exist only for transient time and are rapidly converted to alkyl halides. These intermediates can be isolated only in unusual reaction media such as superacid solvents.[34] On the other hand, a frozen alcohol surface provides a much different reaction environment from liquid solvents mainly for two reasons. Firstly, according to the Arrhenius equation, the thermal rate crossing over an activation barrier is negligible at the temperature of frozen alcohols (<150 K) for the majority of chemical reactions. Secondly, the rate of reagent diffusion is reduced by several orders of magnitude upon the phase transition from liquid to solid in general. With such drastic changes, the occurrence of a chemical reaction in any appreciable speed might be considered doubtful on frozen molecular surfaces.

For a reaction study on a frozen alcohol film, it is necessary to prepare a well-defined and contamination-free surface, since the lack of information about the structure and chemical composition brings a perplex situation to the investigation. An ultra thin film deposited on a metal surface under ultra high vacuum (UHV) is a good candidate for this purpose. In the present work, we examined the reactions depicted in Scheme 1 by preparing ultra thin alcohol films on Ru(001) in UHV. On these surfaces we found that alcohols readily reacted with HBr to produce protonated alcohols and *tert*-butyl cation, despite the hostile nature of the environment mentioned above. The reactions, however, did not go to completion and stopped at intermediate states. The trapped species on the surface were directly identified by the techniques of Cs^+ RIS and low-energy sputtering. This work not only demonstrates how chemistry of alcohol differs on a frozen molecular surface and in a flask, but also gives the first clear example that the intermediates of organic reactions can be isolated on frozen molecular surfaces, a conjecture thus far assumed in interstellar molecular evolution.

Experimental Section

The detailed description of Cs^+ RIS experiment on a frozen molecular surface has been described previously.[28, 32, 33] In the UHV chamber[32] with a base pressure of 1×10^{-10} Torr, a Cs^+ beam was generated from a surface ionization source and was scattered at a sample surface to be analyzed. The Cs^+ beam energy was chosen between 10 and 50 eV, and the current density at the sample was 2–3 nA cm^{-2}. The scattered positive ions were measured with a quadrupole mass spectrometer (QMS; ABB Extrel) with its ionizer filament off. The scattered ions are composed of reflected primaries, RIS products that are association products of Cs^+ with neutral molecules at the surface, and the preexisting ions ejected from the surface. The mechanism of the RIS process on a frozen molecular surface has been explained.[33] The beam incidence and the detector angles both were 45° with respect to the surface normal.

The substrate was a Ru single crystal with a (001) face attached to a sample manipulator, and its temperature could be varied in the range of 90–1500 K. The substrate surface was cleaned by repeated cycles of Ar^+ sputtering and annealing at 1500 K in UHV. Alcohol films were deposited on this surface maintained at 120 K by backfilling the chamber with alcohol vapor at a pressure of $1-5\times10^{-8}$ Torr. C_2H_5OD (Aldrich, 99.5 + % isotope purity) and 2-methylpropan-2-ol (Aldrich, 99.5 + % purity) samples were degassed by several vacuum freeze–thaw cycles before introduced into the chamber. The alcohol films were prepared to the thickness of 3–5 monolayers (MLs), where the thickness was deduced from TPDMS measurements. Calibration experiments on alcohol films of various thickness indicated that 3–5 ML was sufficient to eliminate basically all the substrate effects in the surface reaction. The sampling depth of RIS is one monolayer on frozen molecular films in the employed energy range.[33] Ion-induced damage or surface contamination by incident Cs^+ ions was negligible during the time of RIS spectral acquisition. Whenever necessary, fresh films were prepared to eliminate the surface contamination effects in the measurement. An ethanol film deposited at 120 K is in a plastic-crystalline phase (rotationally disordered phase).[29, 30] The packing structure is unknown for 2-methylpropan-2-ol. HBr gas (Aldrich, 99 + % purity) was introduced into the chamber through a separate leak valve and guided close to the sample face by a tube doser, which reduced chamber contamination by the acid. In this configuration the pressure difference of HBr between the sample and the ionization gauge region was about eight times, which was taken into account in calculating the HBr exposure at the sample. The chamber was equipped with an Auger spectrometer to monitor surface cleanness and elemental composition. Residual gas analysis and TPDMS experiments were done with a QMS.

Results

Reaction on the ethanol surface: A film of deuterated ethanol C_2H_5OD was deposited on Ru(001) at 120 K, and its surface was analyzed with RIS at 100 K. Figure 1a shows an

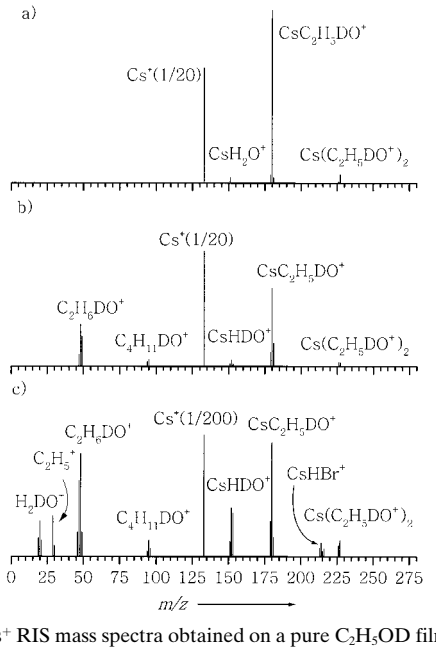

Figure 1. Cs^+ RIS mass spectra obtained on a pure C_2H_5OD film a) and on a C_2H_5OD film exposed to HBr gas for 0.2 L b). Cs^+ beam energy was 20 eV in a) and b). In c), Cs^+ energy was increased to 40 eV on a C_2H_5OD film exposed to 0.2 L of HBr. The ethanol films were 3–4 ML thick, prepared by condensing C_2H_5OD vapor on a Ru(001) substrate at 120 K. HBr gas was added to the films at 100 K. Cs^+ peak intensity is shown in a reduced scale.

  0947-6539/03/0908-1707 $ 20.00+.50/0

RIS spectrum obtained at Cs^+ collision energy of 20 eV. The spectrum shows a strong peak of the reflected Cs^+ primaries at m/z 133, together with RIS products at m/z 180 and m/z 227 which are association products of Cs^+ with neutral molecules at the surface. The m/z 180 peak is assigned as $CsC_2H_5DO^+$, representing the pickup of a C_2H_5OD molecule at the surface by a Cs^+ projectile. The m/z 227 peak, $CsC_4H_{10}O_2D_2^+$, is due to the pickup of two ethanol molecules. In $CsC_2H_5DO^+$ and $CsC_4H_{10}O_2D_2^+$, ethanol is believed to retain its molecular identity, since Cs^+ is unreactive toward ethanol molecule in gas phase and binds to it only through ion–dipole attraction force. In this respect, the ions will be written as $Cs(C_2H_5OD)^+$ and $Cs(C_2H_5OD)_2^+$ in the text whenever structural clarity is needed. The RIS peaks reveal that ethanol exists as an undissociated molecule on the frozen film. A small peak at m/z 151 (CsH_2O^+) is due to adsorption of residual water vapor on the surface, and its intensity increased with time after initial deposition of the film.

In Figure 1b, we added HBr on the C_2H_5OD film for an exposure of 0.2 L (1 L = 1×10^{-6} Torr s) at 100 K, and then examined the surface with RIS at the same temperature. Upon HBr addition, new peaks readily appeared at m/z 48 and 95, in addition to the RIS peaks already seen in Figure 1a. The m/z 48 amu signal is assigned as protonated ethanol ($C_2H_5ODH^+$), and the m/z 95 amu signal, protonated ethanol dimer [$(C_2H_5OD)_2H^+$]. Each of these peaks is accompanied by smaller neighboring peaks of 1 amu difference, indicating that the protonated ethanol undergoes H/D exchange reactions on the surface. For convenience the chemical species will be denoted hereafter only by its representative isotope. It is important to recognize that the $C_2H_5ODH^+$ and $(C_2H_5OD)_2H^+$ signals are due to protonated ethanol molecules produced from reaction of HBr with ethanol on the surface. These preexisting ions are desorbed molecularly by a process called *low-energy sputtering* upon Cs^+ impact.[14, 28]

In Figure 1c, Cs^+ impact energy was increased to 40 eV to analyze the same surface as in Figure 1b. Additional peaks are seen at m/z 20, 29, 213, and 215. The m/z 20 amu peak is assigned as protonated water (H_2DO^+), and the m/z 29 amu peak as $C_2H_5^+$. The RIS products appeared at m/z 213 and 215 correspond to $CsHBr^+$, which indicates that a certain fraction of HBr remains undissociated on the surface.

Further we examined the low-energy sputtered ions observed in Figure 1b and c, by monitoring their intensities as a function of Cs^+ impact energy. Figure 2a shows the intensities of $C_2H_5OHD^+$ and $C_2H_5^+$ ions measured on two different films: one made only of ethanol and the other, HBr added to ethanol. On the HBr/C_2H_5OD surface, the $C_2H_5OHD^+$ signal shows a substantial intensity even at a Cs^+ energy of 10 eV. The $C_2H_5^+$ emission from this surface exhibits a threshold at 15–20 eV. The threshold energies for two ions are obviously different, suggesting that they have different origins. $C_2H_5OHD^+$ with the lower threshold must be due to molecular ejection of preexisting $C_2H_5OHD^+$ ions on the surface. In analogy, low-energy sputtering readily ejects hydronium and ammonium ions from the surfaces containing these preformed ions.[28] The $C_2H_5^+$ signal with the higher threshold, on the other hand, must result from collisional fragmentation of preexisting $C_2H_5OHD^+$. The fragmentation

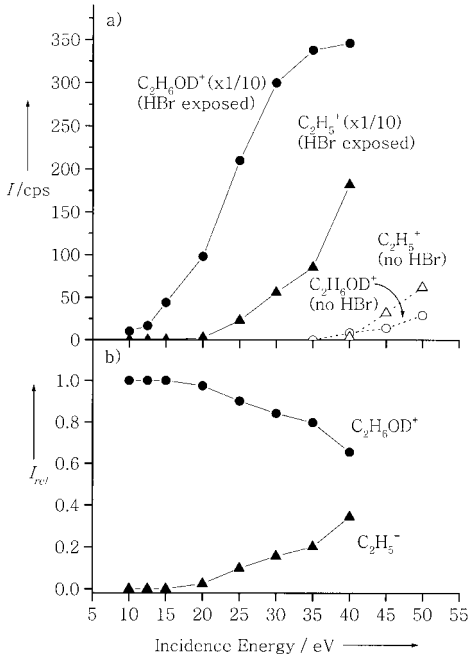

Figure 2. a) Variation of ion intensities with Cs^+ impact energy. Solid symbols represent the signals from an ethanol film exposed to 0.2 L HBr, and open symbols, from a pure ethanol film. The sample temperature was 100 K. b) Relative intensities are plotted for the $C_2H_6OD^+$ and $C_2H_5^+$ signals from the HBr-exposed ethanol surface in a).

of $C_2H_5OHD^+$ produces HDO as well, and this species is evidenced in Figure 1c by the increase in $CsHDO^+$ signal and by the appearance of protonated water signal, H_2DO^+. In Figure 2b, $C_2H_5OHD^+$ and $C_2H_5^+$ signals are plotted against their relative intensity ratio. The relative intensity of $C_2H_5^+$ is negligible at low energy and increases above 20 eV, at the expense of the decay of $C_2H_5OHD^+$ intensity at high energy. This behavior reveals that $C_2H_5^+$ is a secondary species produced from $C_2H_5OHD^+$ fragmentation.

Also shown in Figure 2a are the emission yields of $C_2H_5OHD^+$ and $C_2H_5^+$ from a *pure* ethanol film which does not have preexisting ions. These signals are emitted only at impact energy greater than 40 eV and their yields are very small even above this energy. These ions are produced as a result of *ordinary* sputtering process, that is, impact-induced fragmentation and ionization of neutral molecules. This means that the ions appeared at energy below 40 eV in Figure 1 are due to *low-energy sputtering*, which refers to collisional desorption of preexisting $C_2H_5OHD^+$ ions, either molecularly or in fragments.

The observed threshold energy for ion emission is ultimately related to formation energy of the ion and its binding strength to the surface. Hydrogen-bonding energy of protonated ethanol to another ethanol molecule is 32.2 kcal mol^{-1} from gas-phase measurement.[35a] This value is related to the molecular desorption energy of protonated ethanol from an ethanol film. The formation energy of $C_2H_5^+$ from protonated ethanol in gas phase is 34 kcal mol^{-1},[35b] and this will roughly be the energy additionally required for $C_2H_5^+$ ejection from the surface via fragmentation of protonated ethanol. The adsorption energy difference of protonated ethanol and $C_2H_5^+$ is not included in this estimation, as it is small

0947-6539/03/0908-1708 $ 20.00+.50/0 *Chem. Eur. J.* **2003**, *9*, No. 8

compared to their formation energies. The heterolytic cleavage of a neutral ethanol molecule to $C_2H_5^+$ and OH^- in gas phase requires an energy of 239 kcal mol^{-1},[35c] much higher than the previous two values. These gas-phase values are well correlated with the threshold energies of ion emission in the present study: <10 eV for desorption of protonated ethanol (the gas-phase value is 32.2 kcal mol^{-1}), 15–20 eV for $C_2H_5^+$ emission from a protonated ethanol surface (66 kcal mol^{-1}), and 40 eV for $C_2H_5^+$ production from a pure ethanol film (239 kcal mol^{-1}). The thermodynamic correlation further supports that the threshold energies distinguish the different origins of low-energy sputtered ions. Desorption of protonated ethanol occurs at the lowest impact energy, its fragmentation at a higher energy, and the impact-induced ionization of neutral ethanol requires the highest energy.

Particular attention was given in the present study as to whether ethyl bromide is formed or not. In liquid solvents, protonated ethanol is only a transient intermediate and is readily converted to ethyl bromide through the S_N2 transition state (Scheme 1). In the present case, $CsC_2H_5Br^+$ signal (*m*/*z* 241 and 243) did not appear even after extensive signal accumulation. To check if RIS can quantitatively identify C_2H_5Br on the surface, a calibration experiment was performed in which C_2H_5Br was deposited on a frozen ethanol film and its detection sensitivity was measured. The RIS detection efficiency for C_2H_5Br, that is, the probability that Cs^+ picks up C_2H_5Br adsorbates to form $CsC_2H_5Br^+$, was found to be 1×10^{-3} at Cs^+ energy of 20 eV. From this RIS efficiency, we conclude that the reaction of HBr with ethanol does not form C_2H_5Br in any appreciable amount on the surface (<0.05 ML in Figure 1b). This conclusion is also supported by the observation that the intensity of $CsHDO^+$ signal was hardly increased in Figure 1b from the original CsH_2O^+ intensity in Figure 1a. If the S_N2 reaction occurred, it would form HDO as the coproduct of C_2H_5Br. Note that strong H_2DO^+ and $CsHDO^+$ signals in Figure 1c are due to collisional fragmentation of protonated ethanol at 40 eV, as mentioned before. The negligible increase of $CsHDO^+$ signal from Figure 1a to Figure 1b indicates that the increase in surface water concentration is less than 5×10^{-4} ML, as calculated from the RIS detection efficiency for physisorbed water (about 0.1).[33] This sets an upper limit for the S_N2 reaction yield for C_2H_5Br to be 0.3%, if the initial coverage of HBr is assumed to be 0.2 ML with HBr sticking probability of unity on the surface. In this estimate the small, unionized portion of HBr molecules is ignored. From the almost absent water species on the surface, it can also be said that self-alkylation reaction of ethanol which releases water does not occur either.

The transition state of the S_N2 reaction, C_2H_6DOBr, were it formed and trapped on the surface, would be detected as $CsC_2H_6DOBr^+$ (*m*/*z* 260 and 262). This signal was not observed nor its possible fragmentation peak, $CsC_2H_5Br^+$.

The temperature effect on the reaction was examined by varying the substrate temperature over the range of 100–150 K. Above 150 K an ethanol film sublimes in vacuum. The only change observed was an increase in signal intensity of protonated ethanol by 15% upon a temperature increase from 100 to 150 K. The other features of Figure 1b and c remained unchanged. To examine the temporal behavior of the reaction, we delayed the RIS measurements after adding HBr to the film. The spectral intensities did not change noticeably with the delay time up to 30 min at 100 K.

Reaction on the 2-methylpropan-2-ol surface: Figure 3 shows RIS results obtained on 2-methylpropan-2-ol films. On a pure 2-methylpropan-2-ol film (Figure 3a), the strongest RIS peak observed is $CsC_4H_{10}O^+$ (*m*/*z* 207), which represents the

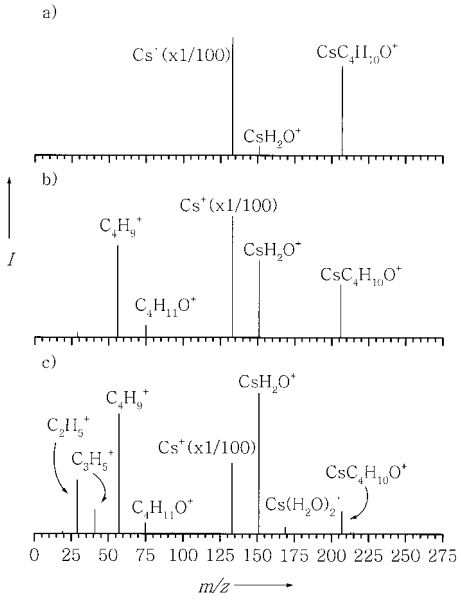

Figure 3. Cs^+ RIS mass spectra obtained on a pure $(CH_3)_3COH$ film a) and on a $(CH_3)_3COH$ film after HBr exposure for 0.3 L b). Cs^+ beam energy was 20 eV. In c), Cs^+ energy was increased to 40 eV on a $(CH_3)_3COH$ film exposed to 0.3 L of HBr. The alcohol films were prepared 4–5 ML thick on Ru(001) at 120 K. HBr exposure and RIS analysis were done at 100 K. Cs^+ peak intensity was reduced by the factor indicated.

pickup of $(CH_3)_3COH$ molecule by Cs^+. No fragmented or ionized species of 2-methylpropan-2-ol is observed in the spectrum. The small CsH_2O^+ signal (*m*/*z* 151) is attributed to physisorption of residual water vapor.

In Figure 3b, 0.3 L of HBr was added to the 2-methylpropan-2-ol film at 100 K, and the resulting surface was analyzed using a 20 eV Cs^+ beam. For low-energy sputtered peaks, $C_4H_9^+$ (*m*/*z* 57) appears strong together with $C_4H_{11}O^+$ (*m*/*z* 75), which are assigned as *tert*-butyl carbocation $[(CH_3)_3C^+]$ and protonated 2-methylpropan-2-ol $[(CH_3)_3COH_2^+]$, respectively. For RIS peaks, CsH_2O^+ signal is much increased in intensity. This increase is not caused by adsorption of residual water nor collisional fragmentation of protonated 2-methylpropan-2-ol by incident beams. The CsH_2O^+ signal appeared strong right from the start of RIS measurement and did not vary significantly with a beam exposure time. The efficient emission of $(CH_3)_3C^+$ and $(CH_3)_3COH_2^+$ ions at this low energy indicates that these ions preexist on the surface, formed by reaction of HBr with 2-methylpropan-2-ol. The surface water molecules represented by CsH_2O^+ must be formed in the conversion reaction of $(CH_3)_3COH_2^+$ to $(CH_3)_3C^+$ depicted in Scheme 1.

  0947-6539/03/0908-1709 $ 20.00+.50/0

When Cs^+ energy was increased to 40 eV in Figure 3c, the spectrum showed additional peaks. In particular, $C_2H_5^+$ (*m*/*z* 29) and $C_3H_5^+$ (*m*/*z* 41) appear in addition to the already observed $C_4H_9^+$ and $C_4H_{11}O^+$. To judge whether these ions are preexisting species or secondary products due to molecular fragmentation, we examined their yields as a function of impact energy, as we did before in Figure 2. Figure 4a shows that $C_4H_9^+$ and $C_4H_{11}O^+$ ions are emitted even at 10 eV, whereas the $C_2H_5^+$ and $C_3H_5^+$ emission exhibits a threshold at 15–20 eV. The relative intensity ratios of these signals are plotted in Figure 4b. The gradual decrease of the $C_4H_9^+$ and

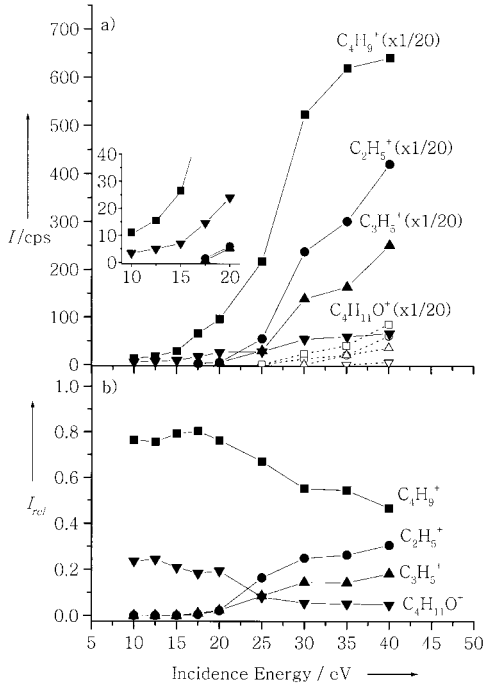

Figure 4. a) Ion intensities as a function of Cs^+ energy. Solid symbols represent the signals from a $(CH_3)_3COH$ film exposed to 0.3 L of HBr, and open symbols, from a pure $(CH_3)_3COH$ film. The sample temperature was 100 K. The inset magnifies the threshold energy region. b) Signal intensities of $C_4H_9^+$, $C_4H_{11}O^+$, $C_2H_5^+$, and $C_3H_5^+$ from the HBr-exposed $(CH_3)_3COH$ film are shown for their relative abundance.

$C_4H_{11}O^+$ curves at higher energy is characteristic of intact desorption of preformed ions. On the other hand, the $C_2H_5^+$and $C_3H_5^+$ curves start from zero to increase gradually for higher energy, indicating that they are produced from fragmentation of $C_4H_9^+$ and $C_4H_{11}O^+$. Shown also in Figure 3a are the emission intensities of the same ions from a *pure* 2-methylpropan-2-ol film. The ion emission is observed only at $>$ 25 eV on this surface with very weak intensity. The difference in the threshold energies and the energy dependency in ion yields prove the preexistence of $C_4H_9^+$ and $C_4H_{11}O^+$ ions on the surface, which are formed in the reaction of HBr with 2-methylpropan-2-ol.

In addition to the peaks shown in Figure 3c, a 40 eV spectrum contains more peaks that have too small intensity to be visible in the displayed scale of Figure 3c. Table 1 summarizes all the peaks observed at 40 eV, together with their relative intensity and classification of their origins (preexisting or fragmented by the collision). The peak origin was deduced from energy dependency of the corresponding signal. In Table 1, H_3O^+ is interpreted to be formed when water molecules, released from protonated alcohol, are protonated by HBr. $CsHBr^+$ is seen at *m*/*z* 212 and 214, which indicates that a small portion of HBr remains undissociated at the surface. $CsC_4H_9Br^+$ appears with a very small intensity at *m*/*z* 269 and 271. Most of the peaks in Table 1 do not vary in intensity with surface temperature (100–150 K) or reaction time (0–30 min), except that $C_4H_{11}O^+$ and $CsC_4H_9Br^+$ signals increase slightly at higher temperature.

Table 1. List of the peaks observed from a $HBr/(CH_3)_3COH$ surface upon 40 eV Cs^+ impact.

m/*z* Peak	Assigned formula	Relative height [%][a]	Origin
19	H_3O^+	1.5	preexisting
29	$C_2H_5^+$	25	fragmented
41	$C_3H_5^+$	11	fragmented
57	$C_4H_9^+$	57	preexisting
75	$C_4H_{11}O^+$	5	preexisting
93	$C_4H_{11}O\cdot H_2O^+$	<0.5	preexisting
151	CsH_2O^+	81	preexisting
169	$Cs(H_2O)_2^+$	4	preexisting
207	$CsC_4H_{10}O^+$	13	preexisting
212, 214	$CsHBr^+$	2	preexisting
269, 271	$CsC_4H_9Br^+$	<0.02	preexisting

[a] The relative peak heights are calculated separately for low-energy sputtered ions (*m*/*z* $<$ 133) and RIS products (*m*/*z* $>$ 133).

We examined the $CsC_4H_9Br^+$ signal in more detail, since this is the end product of the 2-methylpropan-2-ol reaction in liquid. Firstly, to check if RIS can properly detect C_4H_9Br, we adsorbed C_4H_9Br on a new 2-methylpropan-2-ol film and analyzed the surface by RIS. Figure 5a shows a 40 eV spectrum obtained on a pure 2-methylpropan-2-ol film, and Figure 5b, a C_4H_9Br-adsorbed alcohol film. The two spectra show almost identical features, but small extra peaks are seen at *m*/*z* 269 and 271 in Figure 5b, representing $CsC_4H_9Br^+$. This shows that C_4H_9Br is properly detected by RIS and does not

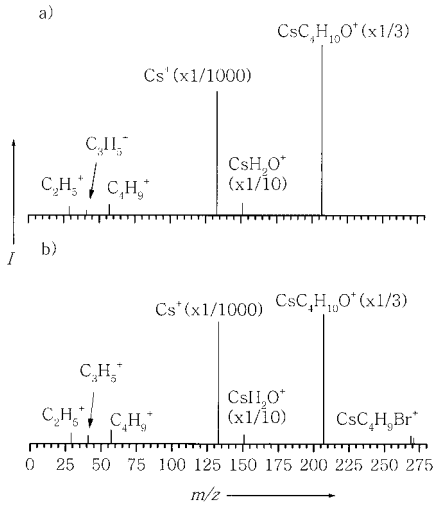

Figure 5. Cs^+ RIS mass spectra from a pure $(CH_3)_3COH$ film a) and from a $(CH_3)_3COH$ film covered with 0.2 ML of C_4H_9Br b). Cs^+ collision energy was 40 eV.

0947-6539/03/0908-1710 $ 20.00+.50/0 *Chem. Eur. J.* **2003**, *9*, No. 8

fragment significantly, as deduced from the unchanged $C_4H_9^+$ intensity. Secondly, we quantitated the RIS detection sensitivity for C_4H_9Br through calibration experiments on 2-methylpropan-2-ol films with various C_4H_9Br coverages. The absolute coverage of C_4H_9Br was estimated from the decay rate of $CsC_4H_{10}O^+$ signal which comes from the underlying alcohol film. A linear calibration plot was obtained for $CsC_4H_9Br^+$ intensity versus C_4H_9Br coverage in the range of 0.05 – 1.0 ML, from which the amount of C_4H_9Br product in Table 1 was estimated to be about 0.005 ML. This value corresponds to the C_4H_9Br formation yield of 2% in the reaction of HBr with a 2-methylpropan-2-ol film. A small portion of unionized HBr remained on the surface was ignored in the yield calculation. The other products of the reaction, *tert*-butyl carbocation and protonated 2-methylpropan-2-ol, have the branching ratio of 78 and 20%, respectively, as deduced from their peak intensities in Figure 3b by assuming that their sputtering efficiencies are the same.

Discussion

According to the results shown in the previous section, the reactions on the frozen alcohol surfaces can be summarized as follows. HBr reacts with an ethanol surface to exclusively produce protonated ethanol. On a 2-methylpropan-2-ol surface, the major species formed are protonated 2-methylpropan-2-ol (20%) and *tert*-butyl cation (78%). A large fraction of the former is transformed to the latter by loss of water. Although both alcohols produce alkyl bromides as the final products in liquid, the yields for alkyl bromides on the cold surfaces are almost negligible ($< 0.3\%$ for ethyl bromide and 2% for *tert*-butyl bromide). It can be noticed that the products identified in this work are the intermediates of the liquid-phase reactions. This gives a good reason to believe that the reaction on a frozen molecular surface has the same reaction path (potential energy surface) as that for liquid alcohol. Molecular constituents are basically the same in both environments. The big difference, however, is whereas a liquid-phase reaction easily finds the lowest energy path of the potential energy surface and goes all the way to final products due to high mobility of the reagents, this is not the case on a frozen film. Scheme 2 summarizes the mechanistic paths on frozen alcohol films based on the present results. In the liquid phase, the reaction of HBr with primary alcohol produces alkyl bromide with a yield typically greater than 80%, and protonated alcohol is never stabilized. On the other hand, the frozen molecular surface blocks the formation of the S_N2 transition state in the ethanol reaction and traps the protonated ethanol intermediate. For the reaction of *tert*-butyl alcohol, the rate-determining step in liquid solvent is heterolytic dissociation of the reactant to a carbocation and the leaving group. The dissociation is followed by rapid combination of the carbocation with a nucleophile present in the medium, forming *tert*-butyl bromide. This S_N1 reaction is governed by thermodynamics. On the cold surface, the heterolytic dissociation of the protonated *tert*-butyl alcohol does occur with a yield of about 78%, but the next process which combines $(CH_3)_3C^+$ and Br^- is prohibited. Note that only *tert*-butyl alcohol goes beyond the protonation step to isolate the carbocation. Therefore, the reactions of primary and tertiary alcohols result in different product distributions on the frozen surfaces, unlike for liquid reactions. Subtle chemical difference of the reagents is highlighted on the cold surface, enhancing selectivity of the reactions.

The intermediates in the S_N1 and S_N2 reactions of alcohols have long been a subject of physical organic chemistry research. These intermediates are too reactive to be stabilized and directly observed in ordinary reaction conditions. Laser flash photolysis studies[36–37] showed that simple alkyl cations have lifetimes shorter than 10^{-10} s in water, methanol, and ethanol solvents at room temperature. Stable carbocations have been isolated in superacid solvents such as SbF_5, and in such environment the first direct observation of *tert*-butyl cation was made by NMR spectroscopy.[38] Since then, various spectroscopic methods[39–42] have yielded information on the structure and reactivity of carbocations, including X-ray photoelectron spectroscopic study of carbocations isolated in a superacid matrix at low temperature.[42] The present study gives the first example of isolating and identifying *tert*-butyl cation and protonated alcohols on a molecular surface that has the same chemical composition as an ordinary medium. The surfaces do not have extremely weak nucleophiles as in superacid solvent, and only the temperature cooling was necessary to isolate the intermediates. Since *tert*-butyl cation is stabilized on the surface but ethyl cation is not, the relative stability of the carbocations appears to go parallel with the gas-phase and liquid-phase trends; this confirms the inherent stability of carbocation outweighs the solvent effect.

We interpret that the isolation of reaction intermediates in this work is a result of kinetic stabilization rather than a thermodynamic consequence, since thermodynamically the reaction paths are identical on a frozen surface and in a liquid medium, as mentioned before. This interpretation is consistent with the observation that the proton transfer in the H_3O^+/NH_3 system is incomplete on water-ice surfaces;[28] the proton-transfer yield is far too small compared to the thermodynamic yield in liquid or gas phase, and is governed by the reagent diffusion on ice. In the present case, close examination of Scheme 2 reveals that the frozen surfaces preferentially stabilize ionic species and prohibit their further reactions. For

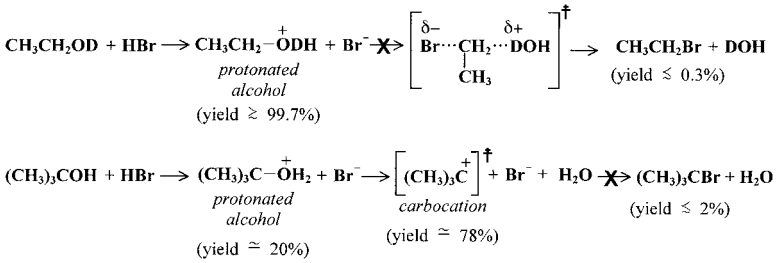

Scheme 2. Summary of the mechanistic paths on frozen alcohol films.

  0947-6539/03/0908-1711 $ 20.00+.50/0

example, protonated alcohols and *tert*-butyl cation are isolated along the reaction paths. Also, the nucleophilic attack of protonated ethanol by Br^- is almost completely blocked, and so is the combination process of *tert*-butyl cation and Br^-. On the other hand, reactions involving movement of neutral molecules are facile, such as the initial reactive encounter of HBr with alcohols producing protonated alcohols and the liberation of water molecule from $(CH_3)_3COH_2^+$.

The preferential stabilization of ionic species in the reaction paths suggests that the reactant mobility is a critical factor which controls the reaction behavior on the cold surface. Ethanol and 2-methylpropan-2-ol molecules are expected to be somewhat mobile on the surface at the employed temperature, since water molecules are known[25, 26] to be so at this temperature on a water-ice film, and the melting temperature of water-ice (273 K) is higher than that of ethanol (159 K) and comparable to 2-methylpropan-2-ol (298 K). Ethanol molecules are expected to be rotationally activated at this temperature on the surface, as they are known[29, 30] to be in the bulk state. Such active diffusion and rotation of alcohol molecules will make their reactive encounters facile. On the other hand, ions such as $C_2H_5OH_2^+$, $(CH_3)_3C^+$, and Br^- are solvated, at least partially, by alcohol molecules on the surface, such that their mobility is greatly reduced. It has been reported[27, 28] that hydronium and ammonium ions are immobile on ice, and the immobility reduces the proton transfer yield from H_3O^+ to NH_3. We believe that such ion immobility prohibits the surface diffusion and attack of a Br^- nucleophile to $C_2H_5OH_2^+$ or $(CH_3)_3C^+$. As such, these ions become trapped between the kinetic barriers. Another factor that may contribute to ion stabilization is the formation of a solvation shell around an ion which has a rigid structure at low temperature. The rigid solvation shell is difficult to be penetrated by a counter ion which is also solvated. In addition, the molecular motions are restricted in two-dimension on the surface. This will hinder formation of a transition state in the optimal three-dimensional geometry. This effect can be particularly serious in the ethanol reaction which requires to form the S_N2 transition state through concerted bond-making and breaking processes.

A few extra points may be mentioned about the kinetic stabilization and its possible consequences. At the temperature of frozen alcohol films, the reaction must be initiated by chemical energy of the reactants since there is not enough thermal energy. The proton affinity of an alcohol provides the driving force for HBr ionization and alcohol protonation. The extra energy released in this step can either be utilized for the next step of carbocation formation or just be dissipated to the surface. Once carbocation or protonated alcohol is formed, they get quenched and trapped almost permanently between the kinetic barriers. In our observation the trapped ions are not transformed to other species up to 30 min at 100 K. Such a feature clearly distinguishes the kinetic trapping from the reduction of thermal reaction speed. The ions trapped on a frozen surface can be regarded as stable products under the given reaction condition, rather than transitory intermediates. The kinetic trapping often results in diverse products compared with those of liquid-phase reactions which are thermodynamically converged, simple species. Also, subtle chemical difference between the reactants can be amplified on a frozen surface to increase the product diversity, as mentioned before. These aspects might have implication for the molecule formation process in interstellar space as proposed[4–10, 23] to take place on the surface of interstellar dust particles covered with ice mantle of simple molecules such as H_2O, CO, CO_2, and CH_3OH. The molecules can break apart upon bombardment by energetic photons or cosmic ray particles to produce reactive fragments. Some reactions may occur solely from chemical energy upon encounter of reactants according to the present finding, but certainly these external energy sources can greatly increase the reaction yield and the range of products. The reactive species created will remain frozen in the cold environment of ice mantle ($T < 50$ K) for some time. Ionic species, if formed, will be isolated for much longer time than neutral species. Such kinetic trapping may help increasing molecular complexity by stabilizing various intermediates and having them available for next reactions.

Conclusion

This work has demonstrated that a low-temperature molecular film provides a unique environment for organic reaction. Simple alcohol molecules do undergo facile reactions with HBr, but their reactivity is quite different from that in the liquid solvent. Reaction of HBr with an ethanol surface produces protonated ethanol as the final product. On a 2-methylpropan-2-ol surface, the major products observed are protonated 2-methylpropan-2-ol and *tert*-butyl cation. Alkyl bromides are hardly formed in both reactions, although they are exclusive final products in the reactions in liquid solvents. Unique features of the frozen surface reactions can be summarized as follows: i) the reactions are controlled by kinetics rather than by thermodynamics, ii) the kinetic control leads to isolation of reaction intermediates, iii) ionic species are preferentially stabilized in the reaction path, and iv) the reactivity of primary and tertiary alcohols is well distinguished.

A molecular interpretation is suggested for these observations in terms of reactant mobility. While neutral alcohol molecules are mobile and rotationally activated on the surface, ion mobility is greatly reduced due to partial solvation of an ion by alcohol molecules. The reduced ion mobility prohibits the diffusive encounter between Br^- and a counter ion such as $C_2H_5OH_2^+$ and $(CH_3)_3C^+$, thus effectively blocking the completion of the S_N1 and S_N2 pathways. Other factors that may additionally contribute to the ion trapping include the rigid solvation shell formed around an ion, and the two-dimensional restriction in forming the optimal geometry of the transition states.

Acknowledgement

This work was supported by the Basic Research Program of the Korea Science & Engineering Foundation (R02-2002-000-00005-0).

[1] M. J. Molina, T. L. Tso, L. T. Molina, F. C. Y. Wang, *Science* **1987**, *238*, 1253.
[2] M. A. Tolbert, M. J. Rossi, R. Malhotra, D. M. Golden, *Science* **1987**, *238*, 1258.

  0947-6539/03/0908-1712 $ 20.00+.50/0

[3] D. R. Hanson, A. R. Ravishankara, *J. Phys. Chem*. **1992**, *96*, 2682.
[4] A. G. G. M. Tielens, S. B. Charnley, *Origins Life Evol. Biosphere* **1997**, *27*, 23.
[5] For a recent review on this subject, see: J. M. Greenberg, *Surf. Sci*. **2002**, *500*, 793.
[6] A. Lager, J. L. Puget, *Astron. Astrophys. Lett*. **1984**, *137*, L25.
[7] D. C. B. Whittet, W. A. Schutte, A. G. G. M. Tielens, A. C. C. A. Boogert, Th. de Graauw, P. Ehrenfreund, P. A. Gerakines, F. P. Helmich, T. Prusti, E. F. van Dishoeck, *Astron. Astrophys.* **1996**, *315*, L357.
[8] W. Hagen, L. J. Allamandola, J. M. Greenberg, *Astrophys. Space Sci.* **1979**, *65*, 215.
[9] P. A. Gerakines, W. A. Schutte, P. Ehrenfreund, *Astron. Astrophys.* **1996**, *312*, 289.
[10] M. P. Bernstein, S. A. Sandford, L. J. Allamandola, J. S. Gillette, S. J. Clemett, R. N. Zare, *Science* **1999**, *283*, 1135.
[11] J. D. Graham, J. T. Roberts, *J. Phys. Chem*. **1994**, *89*, 5974.
[12] H. A. Donsig, J. C. Vickerman, *J. Chem. Soc. Faraday Trans.* **1997**, *93*, 2755.
[13] J. E. Schaff, J. T. Roberts, *Langmuir* **1998**, *14*, 1478.
[14] H. Kang, T.-H. Shin, S.-C. Park, I. K. Kim, S.-J. Han, *J. Am. Chem. Soc.* **2000**, *122*, 9842.
[15] S. Haq, J. Harnett, A. Hodgson, *J. Phys. Chem. B* **2002**, *106*, 3950.
[16] J. P. Devlin, N. Uras, J. Sadlej, V. Buch, *Nature* **2002**, *417*, 269.
[17] A. B. Horn, T. B. Roddis, N. A. Williams, J. R. Sodeau, *J. Chem. Soc Faraday* **1998**, *94*, 1721.
[18] A. B. Horn, J. R. Sodeau, T. B. Roddis, N. A. Williams, *J. Phys. Chem. A* **1998**, *102*, 6107.
[19] M. A. Zondlo, S. B. Barone, M. A. Tolbert, *J. Phys. Chem. A* **1998**, *102*, 5735.
[20] S.-H. Lee, D. C. Leard, R. Zhang, L. T. Molina, M. T. Molina, *Chem. Phys. Lett.* **1999**, *315*, 7.
[21] B. Fluckiger, L. Chaix, M. J. Rossi, *J. Phys. Chem. A* **2000**, *104*, 11739.
[22] M. T. Sieger, W. C. Simpson, T. M. Orlando, *Nature* **1998**, *394*, 554.
[23] M. E. Palumbo, G. Strazzulla, Y. J. Pendleton, A. G. G. M. Tielens, *Astrophys. J.* **2000**, *534*, 801.
[24] Summary: T. E. Madey, R. E. Johnson, T. M. Orlando, *Surf. Sci*. **2002**, *500*, 838.
[25] S. M. George, F. E. Livingston, *Surf. Rev. Lett.* **1997**, *4*, 771.
[26] D. E. Brown, S. M. George, *J. Phys. Chem*. **1996**, *100*, 15460.
[27] J. P. Cowin, A. A. Tsekouras, M. J. Ledema, K. Wu, G. B. Ellison, *Nature* **1999**, *398*, 405.
[28] S.-C. Park, K.-W. Maeng, T. Pradeep, H. Kang, *Angew. Chem.* **2001**, *113*, 1545; *Angew. Chem. Int. Ed.* **2001**, *40*, 1497.
[29] F. J. Bermejo, A. Criado, R. Fayos, R. Fernadez-Perea, H. E. Fischer, E. Suard, A. Guelylah, J. Zuniga, J. *Phys. Rev. B* **1997**, *56*, 11536.
[30] A. Criado, M. Jimenez-Ruiz, C. Cabrillo, F. J. Bermejo, R. Fernandez-Perea, H. E. Fischer, F. R. Trouw, *Phys. Rev. B* **2000**, *61*, 12082.
[31] J. D. Graham, J. T. Roberts, *Langmuir* **2000**, *16*, 3244.
[32] a) M. C. Yang, C. H. Hwang, H. Kang, *J. Chem. Phys.* **1997**, *107*, 2611; b) S.-J. Han, C.-W. Lee, C.-H. Hwang, K.-H. Lee, M. C. Yang, H. Kang, *Bull. Korean Chem. Soc.* **2001**, *22*, 883.
[33] J. R. Hahn, C.-W. Lee, S-J. Han, R. J. W. E. Lahaye, H. Kang, *J. Phys. Chem. A* **2002**, *106*, 9827.
[34] Summary: G. A. Olah, P. v. R. Schleyer in *Carbonium Ions*, *Vols. I–V*, Wiley, New York, **1968–1976** and reviews therein.
[35] a) D. S. Bomse, J. L. Beauchamp, *J. Am. Chem. Soc.* **1981**, *103*, 3292; b) calculated from: $[\Delta H_f^0(H_2O)+\Delta H_f^0(C_2H_5)+IP(C_2H_5)]-[\Delta H_f^0(C_2H_5OH)+\Delta H_f^0(H^+)+PA(C_2H_5OH)]$; c) calculated from: $D^0(C_2H_5\text{-}OH) - IP(C_2H_5) - EA(OH)$. All thermochemical values for the calculations are from National Institute of Standards and Technology Chemistry Web Book. http://webbook.nist.gov/chemistry (accessed June 2002).
[36] Y. Chiang, A. J. Kresge, *Science* **1991**, *253*, 395.
[37] R. A. McClelland, *Tetrahedron* **1996**, *52*, 6823.
[38] G. A. Olah, W. S. Tolgyesi, S. J. Kuhn, M. E. Moffatt, I. J. Bastein, E. B. Baker, *J. Am. Chem. Soc*. **1963**, *85*, 1328.
[39] G. A. Olah, *Angew. Chem.* **1973**, *85*, 183; *Angew. Chem. Int. Engl. Ed.* **1973**, *12*, 173.
[40] D. G. Farnum, *Adv. Phys. Org. Chem.* **1975**, *11*, 123.
[41] H. Vancik, D. E. Sunko, *J. Am. Chem. Soc*. **1989**, *111*, 3742.
[42] G. A. Olah, G. D. Mateescu, J. L. Riemenschreider, *J. Am. Chem. Soc*. **1972**, *94*, 2529.

Received: October 30, 2002 [F4541]

  0947-6539/03/0908-1713 $ 20.00+.50/0